Application of hydroxyapatite nanoparticles (n-HA) in tumor-associated bone segmental defect

13 August 2019, by Thamarasee Jeewandara

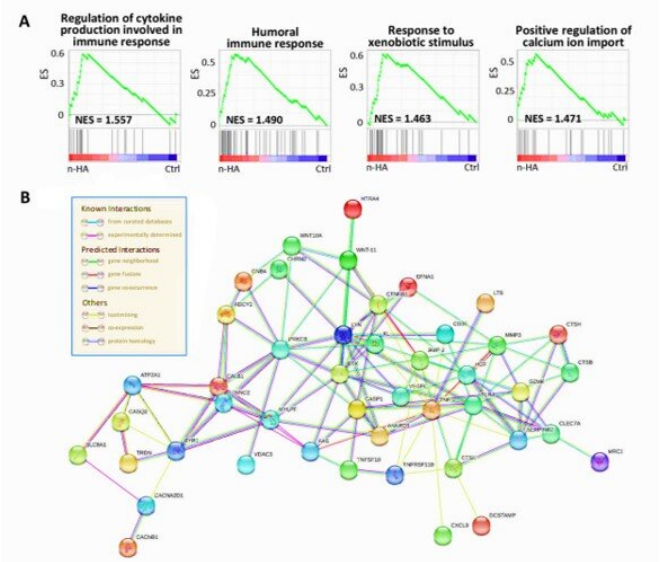

GSEA (Gene Set Enrichment Analysis) and protein-protein interaction analysis. (A) Gene set enrichment analysis of the regulated gene pathways using GO database. The positive enrichment plots of n-HA treated tumor tissue versus control tumor tissue (Ctrl). NES (normalized enrichment score). (B) STRING (v10.5, http://string-db.org) protein-protein interaction networks of distinct proteins. Network nodes represent proteins. Colored nodes, query proteins and first shell of interactors; white nodes, second shell of interactors; empty nodes, proteins of unknown 3D structure; filled nodes, some 3D structure is known or predicted. Edges represent protein-protein associations. Credit: Science Advances, doi: 10.1126/sciadv.aax6946

Materials scientists widely incorporate hydroxyapatite (HA) for bone repair in bone tissue engineering (BTE) due to its superior biocompatibility as a natural component of human bones and teeth. In a recent report on *Science Advances*, a research team highlighted the proliferation-suppressive effect of HA nanoparticles (n-HA) against a variety of cancer cells by combining the translational value of n-HA as a bone-regenerating material and an anti-tumor agent. In the study, Kun Zhang and an interdisciplinary research team in the departments of Orthopedic Surgery, Dermatology, Biomedical Metal Materials and the National Engineering Research Center for Biomaterials in China, demonstrated the inhibition of tumor growth, metastasis prevention and the enhancement of the survival rate in tumor-bearing rabbits treated with n-HA.

They confirmed activation of the mitochondrial-dependent apoptosis pathway in vivo and observed a stimulated immune response to n-HA induced antitumor effects. The research team then loaded a porous titanium scaffold with n-HA and implanted it into a critical-sized segmental bone defect in a rabbit tumor model for translational studies. Based on the results, they verified the ability of the n-HA releasing scaffold to suppress tumor growth and osteolytic lesion while promoting bone regeneration. The research findings provide a strong rationale to use n-HA to regenerate tumor-associated bone segmental defects in vivo.

In the United States, approximately 2,500 new cases of primary bone cancer are diagnosed annually with approximately half the patients exhibiting bone metastasis. During standard clinical treatment of bone cancers, the surgical approach includes resection and reconstruction of the affected bone, followed by adjuvant radiation or chemotherapy. Although load-bearing artificial implants are currently adopted in clinical practice, poor implant-bone osseointegration and the difficulty of new bone formation in a tumor environment remain major challenges for orthopedic surgeons. Incomplete surgical resection of the affected tissue can also risk the spread of tumor cells to result in 8 percent recurrence or

metastases. As a result, researchers urgently aim to develop an implant that combines antitumor activity and bone regeneration functions.

Since the 1970s, clinicians have applied HA-based biomaterials clinically during orthopedic and dental repair. Materials scientists have also developed surfaces modified with HA as prosthetic metal implants for enhanced bone integration. Notable research studies have shown the capacity of n-HA to inhibit cancer cell proliferation and induce apoptosis, including osteosarcoma cells, breast cancer cells, colon cancer cells and liver cancer cells, while sparing normal cells. Preceding studies provided insight to the mechanism of n-HA antitumor activity based on in vitro experiments, although much remains to be known of the underlying mechanism in vivo.

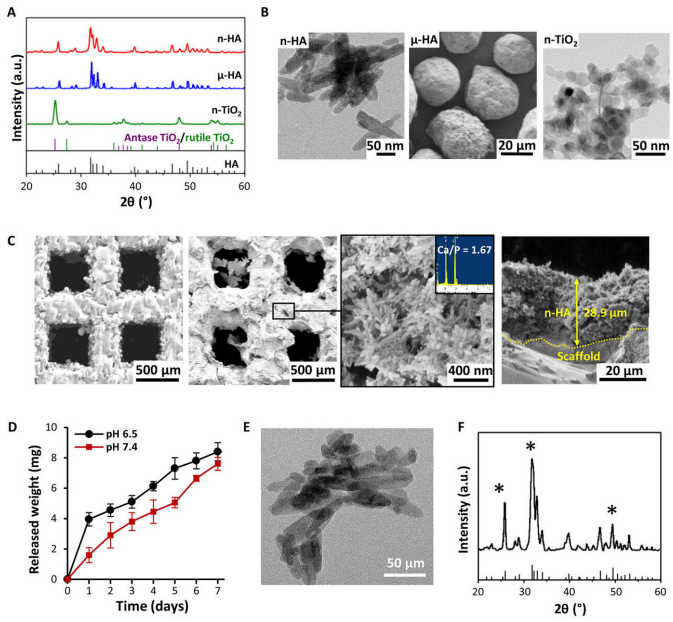

Characterization of particles and scaffold. (A) XRD (X-ray diffraction) patterns of n-HA, ?-HA, and n-TiO2 particles. The standard spectra of HA, anatase TiO2, and rutile TiO2 are given below. a.u., arbitrary units. (B) Representative TEM image of n-HA, SEM image of ?-HA, and TEM image of n-TiO2. (C) SEM images of 3D-printed porous titanium scaffold subjected to acid-alkali treatment, coated with n-HA and surface/cross-sectional alignment of n-HA with EDS confirmation. The dotted yellow line indicates the interface between n-HA coating and scaffold. The yellow arrow marks the average thickness of n-HA layer. Ca/P indicates atomic molar ratio of the selected region. (D) Weight change of particles released from n-HA/scaffolds immersed in tris-HCl solution for 7 days. Error bars represent SD. n = 3 replicates. (E) Representative TEM image of the released n-HA particles. (F) XRD pattern of the released n-HA particles. The asterisk indicates characteristic peaks of HA. Credit: Science Advances, doi: 10.1126/sciadv.aax6946

Testing the new experimental strategy in the lab

In the present work, Zhang et al. presented an unprecedented strategy to combine bone tumor treatment using a 3-D printed titanium scaffold modified with n-HA for antitumor function. They conducted in vitro co-culture experiments first, to demonstrate the ability of the synthetic, rod-shaped n-HA to induce apoptosis in the malignant VX2 tumor cells. Thereafter, the research team implemented an intramuscular tumor model in immunocompetent rabbits to show the suppression of tumor development and reduced metastasis.

Researchers initially observed and reported the anti-tumor effect of n-HA in 1993, when they serendipitously found a control group of pure n-HA to inhibit Ca-9 cancer cell lines further validated in 2003 using functional studies in vitro. In the present work, Zhang et al. used μ-HA and n-TiO_2 particles as control groups alongside n-HA to determine if the antitumor effect originated from the material composition or particle size. For this, they used X-ray diffraction analysis (XRD) and confirmed similarities of the HA phase composition between n-HA and μ-HA. Then using transmission electron microscopy (TEM) images they revealed the rod shape of n-HA and used scanning electron microscopy (SEM) micrographs to observe μ-HA.

They then engineered porous titanium scaffolds using selective laser sintering to satisfy the load-bearing requirements for rabbit cortical bone replacement. Zhang et al. enhanced the bioactivity of the printed scaffolds using acid-alkali treatment and achieved n-HA coating using a combined method of slurry foaming and impregnation. The scientists characterized (tested) the scaffolds to determine the surface chemistry and kinetics of n-HA release in an acidic environment.

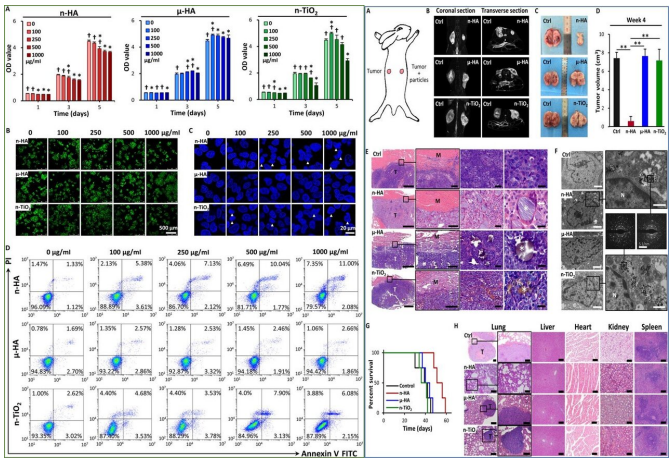

LEFT: In vitro tumor cell viability and apoptosis cocultured with different particles. (A) VX2 cells viability determined by CCK-8 assay when cocultured with n-HA, ?-HA, and n-TiO2 for 1, 3, and 5 days. Error bars represent SD. *P

Testing the biocompatibility and cancer cell apoptosis with different particles.

To test in vitro antitumor activity and toxicity of the particles, the researchers chose a wide range of n-HA concentrations to co-culture with VX2 tumor cells or normal L929 fibroblast cells. During prolonged experiments n-HA reduced the viability of tumor cells, although comparatively, µ-HA did not reduce the viability of either cell type, while n-TiO_2 decreased the viability of VX2 and inhibited L929 cell growth with prolonged time.

When Zhang et al. tested the in vivo antitumor ability of n-HA, they used an intramuscular VX2 tumor model on both flanks (right and left) of the rabbit, and administered n-HA, µ-HA and n-TiO_2 on either side. By week three, they used magnetic resonance imaging (MRI) of individual animals to show reduced HA-treated tumor size in the right hand side, compared to the control in the left hand side. Comparatively neither µ-HA nor n-TiO_2 showed tumor growth suppression in vivo during the same period.

The scientists harvested the tumor samples at week 4 to confirm the antitumor ability of n-HA using histological staining at the interface of the tumor and muscle tissue. They noted diverse immune cells surrounding the n-HA particles, such immune diversity was not observed surrounding µ-HA and n-TiO_2 coated scaffolds. Using TEM observations, Zhang et al. showed both n-HA and n-TiO_2 internalized within tumor cells. Histological findings at week 4 indicated the prevention of metastasis to the lung with n-HA animal groups, although similar observations were not recorded with µ-HA or n-TiO_2. Metastasis elimination in rabbits treated with n-HA led to longer survival rates and lower rates of tumor positive cells compared to those treated with other materials.

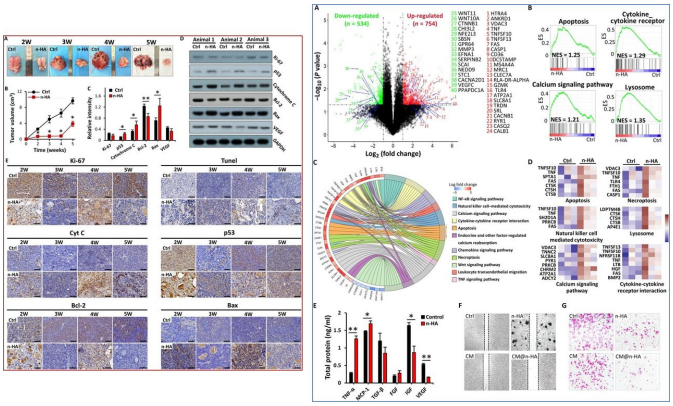

LEFT: Activation of mitochondrial apoptosis pathway by n-HA. (A) Longitudinal observation of the excised tumor treated with n-HA from weeks 2 to 5 (2W to 5W). Ctrl, left flank control without any treatment. (B) Quantification of the excised tumor volume. Error bars represent SD. n = 4 per group. (C and D) Expressions of mitochondrial apoptosis-related markers in tumor tissues measured by Western blotting (WB) at week 4. VEGF, vascular endothelial growth factor; GAPDH, glyceraldehyde phosphate dehydrogenase. Error bars represent SD. n = 3 per group. (E) Immunohistochemical analyses of Ki-67, Cyt C, p53, Bcl-2, and Bax and TUNEL assay of tumor tissues treated with n-HA at week 5 in comparison with control. Scale bar, 50 ?m. *P 2 and a P value of 2 and a P value of